Dusty plasma experiment to confirm an expression for the decay of autocorrelation functions

Zach Haralson* and J. Goree
Department of Physics and Astronomy, The University of Iowa, Iowa City, Iowa 52242, USA

Roman Belousov
The Rockefeller University, New York, New York 10065, USA

(Received 5 July 2017; revised manuscript received 23 February 2018; published 8 August 2018)

Statistical physicists recently proposed an expression for an autocorrelation function (ACF) [Belousov and Cohen, Phys. Rev. E **94**, 062124 (2016)] that has, until now, not been tested experimentally. The expression captures the early behavior of the ACF decay, when the ACF is flattened. Using experimental data from a nonequilibrium steady-state dusty plasma, we confirm that the expression's use extends to liquidlike strongly coupled plasmas. A transition in the shape of the ACF is identified, and we suggest that it corresponds to the onset of collisional scattering.

DOI: 10.1103/PhysRevE.98.023201

I. INTRODUCTION

Time autocorrelation functions (ACFs) of fluctuating quantities are often used to describe microscopic behavior in gases, liquids, and plasmas, including strongly coupled plasmas. In all these physical systems, quantities such as particle velocity, shear stress, or energy current can fluctuate spontaneously due to collisions among individual particles. Calculating an ACF for these quantities requires particle-level data, which are commonly available in computer simulations [1]. Such fine resolution is rarely accessible in experiments. However, for a strongly coupled dusty plasma, like the one we analyze here, the particle-level data can be measured.

The term "strong coupling" describes the condition in a plasma when the average potential energy of a charged species exceeds the thermal kinetic energy. A strongly coupled plasma can behave like a liquid or solid [2]. Generally, the species that can most easily become strongly coupled is the heaviest one, such as ions in the case of an ultracold plasma [3] or warm dense matter [4]. The heaviest species in a dusty plasma experiment like ours consists of small particles of solid matter, which can be strongly coupled due to their great mass and large charge.

Besides laboratory experiments like ours, dusty plasmas are found naturally in the interstellar medium, comet tails, and planetary rings [5,6]. Dusty plasmas also occur in semiconductor manufacturing plasmas [7] and fusion plasmas [8] where they pose a contamination problem. In most of these dusty plasmas, the solid particles can be observed by video imaging, because they are large enough to scatter light copiously. Such imaging yields particle-level measurements of microsphere positions and velocities, which enables the calculation of an ACF that describes the microscopic stochastic behavior.

For all kinds of physical systems with stochastic behavior, a prominent feature in an ACF is its initial decay, which precedes the typical oscillatory and noisy observations at longer times. This decay has thus far usually been described [9–12] by a simple exponential curve $C(t) = C(0)\exp(-t/\tau)$. This description of an ACF can be derived from a first-order Onsager-Machlup fluctuation theory [13]. Unlike this simple exponential curve, though, most instances of ACFs are flattened initially, i.e., for $t \to 0$. The exponential description fails to capture this initial decay of ACFs at short times [12].

An appropriate function to describe this initial decay was needed, as recognized by Belousov and Cohen (BC), who recently derived the formula [14]

$$C(t) = C(0)\exp\left(-\frac{at}{2}\right)\left[\cosh\left(\frac{dt}{2}\right) + \frac{a}{d}\sinh\left(\frac{dt}{2}\right)\right]. \tag{1}$$

This expression is intended to be applicable to many kinds of fluctuating quantities in substances that are dominated by collisions. Equation (1) was derived theoretically for classical equilibrium and nonequilibrium systems by BC, from a generalized second-order fluctuation theory of Machlup and Onsager [15]. The latter describes irreversible processes, taking into account inertia, i.e., resistance of a physical system to forced changes of its state. At this point, experimental tests of Eq. (1) are lacking.

The only test of any kind thus far, for Eq. (1), was a fit to simulation data, reported by BC alongside their theory [14]. They performed a molecular dynamics simulation of a simple fluid. Among the many fluctuating quantities in such a system that allow the calculation of an ACF, they chose the shear stress, which we define below. They confirmed that Eq. (1) fits their shear-stress ACF much better, especially at short times, than does a simple exponential.

In this paper, as our main result we report an experimental confirmation of the theoretically predicted Eq. (1). We verify that the flattened shape at the beginning of the decay, as well as the nearly exponential decay at longer times, are both well described by Eq. (1). To do this, we use data from the experiment of Ref. [16], with a strongly coupled dusty plasma in a liquidlike state.

*zachary-haralson@uiowa.edu

In the experiment [16], the strongly coupled species was a collection of about 6000 solid polymer microspheres, which gained a large negative charge. The other charged species were singly ionized argon ions and electrons; neutral argon atoms were also present and applied a frictional drag force to the microspheres. The microspheres were electrically levitated in a single horizontal layer, with minimal out-of-plane motion, so that their behavior was mainly two dimensional (2D). The microspheres also experienced a shielded electric repulsion with each other, and this collisional behavior was responsible for stochastic particle motion at a microscopic level. For the collection of microspheres, video microscopy allowed particle tracking so that we could obtain the shear stress and its ACF.

The microspheres in our experiment comprised a nonequilibrium steady state. This is because the microspheres constantly received energy from the ion flow (and also from an external laser-heating manipulation in some of our experimental runs), while simultaneously losing energy by friction on the neutral gas. The balance of these energy inputs and losses to the microsphere species determined its steady-state kinetic temperature. Despite these nonequilibrium processes, the collection of microspheres had several steady attributes, including an absence of macroscopic gradients and flows, a velocity distribution that was nearly Maxwellian, and a level of temperature fluctuations (for a small subset of the microspheres) that was nearly the same as expected for a canonical ensemble in thermal equilibrium [17].

II. EXPERIMENT

We now summarize some key conditions of the experiment, which was described in greater detail in Refs. [16,17]. After igniting a radio-frequency powered argon plasma at a pressure of 6 mTorr, we introduced the melamine formaldehyde microspheres. These microspheres were monodisperse, with a diameter 8.7 μm and mass $m = 5.2 \times 10^{-13}$ kg, as specified by the manufacturer. The microspheres settled into a single horizontal layer above the powered electrode. The same collection of microspheres was used for all the experimental runs. The primary data acquisition instrument was a top-view camera that recorded particle motion at 70 frames/s. From the recorded videos, we obtained microsphere positions using a moment method [18] and velocities with particle tracking velocimetry [19,20]. Each video consisted of 4382 frames, corresponding to a length of 62.6 s. We also used a side-view camera to verify that out-of-plane motion was negligible.

In two runs, the collection of microspheres was settled into a crystalline ground state, which allowed obtaining required parameters. To calculate interparticle forces we require the microsphere charge Q and the screening length λ for the Yukawa interaction potential. We obtained these two quantities using a standard phonon analysis of the random motion of microspheres in the lattice [21–23]. The parameter Q drifted slightly from $-15\,500e$ for a run at the beginning of the experiment to $-15\,900e$ at the end [24], while λ drifted from 0.38 to 0.42 mm. In our analysis we take this small drift into account by interpolating linearly between the starting and ending conditions [17]. Other parameters obtained from the analysis of the crystal include the areal density n, the 2D Wigner-Seitz radius $a = (\pi n)^{-1/2}$, the screening length $\kappa = a/\lambda$, and the nominal 2D dusty plasma frequency $\omega_{pd} = (Q^2/2\pi\epsilon_0 ma^3)^{1/2}$. At the start of the experiment these values were $a = 0.307$ mm, $\kappa = 0.72$, and $\omega_{pd} = 86$ s^{-1}, while at the end they were 0.298 mm, 0.78, and 92 s^{-1}.

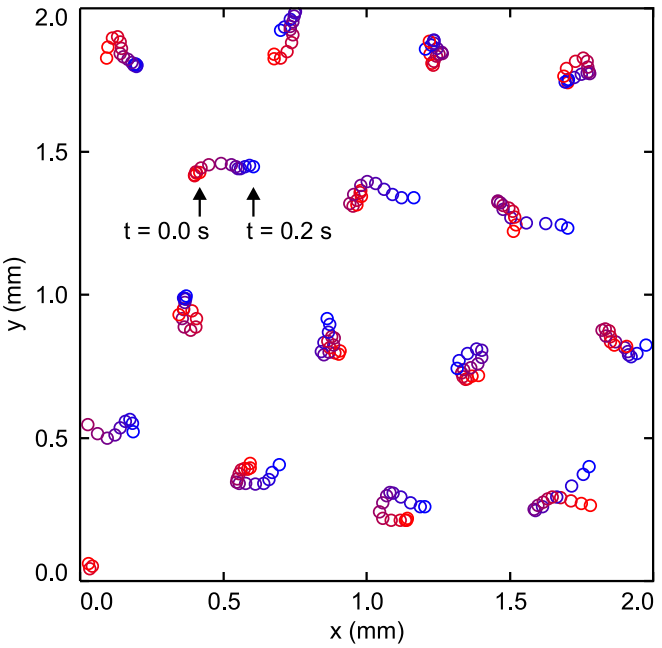

FIG. 1. Experimentally measured microsphere trajectories, under liquidlike conditions. The data points are the positions of microspheres in 15 successive video frames. The shading indicates the passage of time. A significant fraction of the microspheres are seen to be deflected after only four video frames, and a few are already deflected by the third frame. Data points shown here (for a run at $T = 96\,800$ K) were recorded at intervals of 0.014 s. Microsphere positions and velocities from trajectories like these were used to calculate shear stress autocorrelation functions. The region analyzed in the experiment was 15×21 mm, larger than the representative portion shown here.

In eight other runs, which provide our main results, the crystal was melted by applying laser heating to attain a liquidlike state. Two laser beams, operated with a constant power, were scanned over the monolayer, using the pattern of Ref. [25]. These beams imparted momentum to the microspheres [26], increasing the kinetic energy more than 100-fold above the level in a crystalline lattice. The kinetic temperature T of the microspheres was obtained from image analysis data by computing the mean-square velocity. The temperature varied from one run to another according to the applied laser power, with T ranging from $1.1T_{\rm melt}$ to $1.5T_{\rm melt}$, where $T_{\rm melt}$ is the melting temperature from Ref. [27]. The corresponding dimensionless Coulomb coupling parameter $\Gamma = (Q^2/4\pi\epsilon_0 ak_B)/T$ ranged from 139 to 104. The two heating laser beams were balanced to minimize any macroscopic gradients or flows of microspheres. In our test of Eq. (1), we use the eight runs from Refs. [16,17] that had no manipulation besides the laser heating. For brevity, in this paper we will present results from two of these runs; the other six runs are presented in Supplemental Material [28].

For our liquidlike monolayer, microsphere trajectories are shown in Fig. 1. Each data point represents a measured position of a microsphere in one video frame. The trajectories are

portrayed by superimposing the positions for 15 frames (a time interval of 0.2 s). As expected in a liquid, the position of a microsphere wanders stochastically, with a displacement typically ranging from about $0.15a$ to $0.6a$ in this time interval. We note that the shape of the trajectories, while often nearly a straight line for the first few frames, always becomes deflected well before the end of the 15 frames shown.

III. ANALYSIS

Our analysis of the particle tracking data yields the autocorrelation function for shear stress, using the same two steps as in Ref. [16]. While this paper uses the same ACF data as presented in Ref. [16], here we use it for an entirely different purpose. In Ref. [16], ACF data were obtained only as one step toward calculating the viscosity parameter through the Green-Kubo method, whereas here we focus on the shape of the ACF itself, in order to show consistency with the theory of BC. Next we briefly review the analysis necessary to obtain the shear stress ACF, as also described in Ref. [16].

First, we obtained a time series of shear stress P_{xy} in our monolayer from the time series of microsphere positions and velocities. The instantaneous value of this shear stress within a region of area A is computed as

$$P_{xy} = \frac{1}{A}\sum_i \left[m v_{i,x} v_{i,y} - \frac{1}{2}\sum_{j\neq i} |x_j - x_i| \nabla \Phi_{ij} \cdot \hat{y} \right], \quad (2)$$

where v_i is the velocity of particle i interpolated to the same time as the position data x_i and y_i, whereas the subscripts x and y indicate vector components [29]. The potential Φ_{ij}, between particles i and j that were separated by r_{ij}, was obtained from the Yukawa (Debye-Hückel) expression $\Phi_{ij} = (Q^2/4\pi\epsilon_0)\exp(-r_{ij}/\lambda)/r_{ij}$. The Yukawa potential has been experimentally validated [30] in a monolayer dusty plasma like ours. The screening length λ arises physically from the electrons and ions that surround a microsphere.

Second, the ACF for shear stress, $C(t)$, was computed from the time series of P_{xy} as

$$C(t) = \langle P_{xy}(t_0) P_{xy}(t_0 + t) \rangle. \quad (3)$$

The brackets represent a mean, averaged over all possible starting times t_0. The error bar on the value of $C(t)$ is obtained as the corresponding standard deviation of the mean. This error bar does not take into account systematic errors due to uncertainties in the values of Q and λ. Using Q and λ values from the extreme edges of their uncertainty ranges [17] produces only a $\pm 3\%$ shift in the entire ACF curve. A further possible source of error is uncertainty in particle position and velocity measurements, but these uncertainties are so small as to have a negligible effect on P_{xy} and its ACF.

IV. RESULTS

Results for the experimental ACF are shown in Fig. 2. Smooth curves are fits to the theoretical expression, Eq. (1), and to a simple exponential decay. Our video camera's frame rate determined the time step, 0.014 s, between the experimental ACF data points in Fig. 2. Beyond the initial decay in the 0.20-s time range of Fig. 2, the ACF consists mostly of noise centered about zero, not shown here.

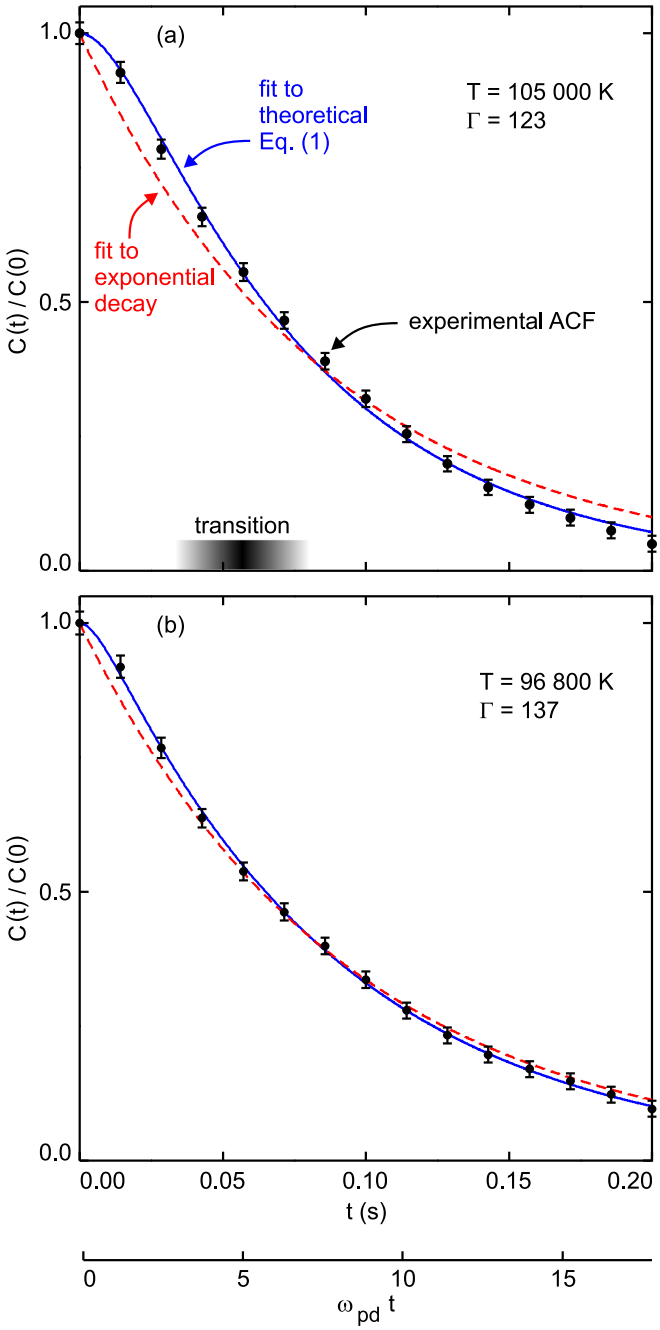

FIG. 2. Shear stress autocorrelation function (ACF). An experimental ACF, obtained from Eq. (3), is presented as a series of data points. At short times, $t \lesssim 0.02$ s, the ACF is flattened, and not exponential; this shape is captured well by the theoretical Eq. (1). Time is indicated in both experimental and normalized units. The lower panel is for the same experimental run as in Fig. 1, while the upper panel is for a different run. Fit parameters for Eq. (1) are (a) $a = 82\ \mathrm{s}^{-1}$ and $d = 53\ \mathrm{s}^{-1}$ and (b) $a = 174\ \mathrm{s}^{-1}$ and $d = 150\ \mathrm{s}^{-1}$.

We find that the theoretical expression of BC, Eq. (1), fits our experimental data very well. This fit, shown as a solid curve in Fig. 2, passes through the error bars of most of the experimental data points. Of particular interest, the expression of BC accurately captures the flattening of the ACF at short times.

A simple exponential, on the other hand, never fits the experimental ACF data well. Compared to this exponential, which is plotted as a broken curve in Fig. 2, our experimental data show an excess correlation at short times, where the ACF is flattened. This same excess correlation and flattening was observed also in the simulation data of BC. The degree to which an exponential fit fails varied from one run to another. Results for other runs are shown in Supplemental Material [28], along with values of $C(0)$.

The behavior of the ACF gradually transitions from excess correlation at early times to a nearly exponential decay later. Examining the ACF curves, we find that this transition occurs generally between $\omega_{pd}t = 3$ and 7, and at the end of this transition the two fit curves usually cross. This transition time range is marked on the lower axis of Fig. 2(a).

In presenting their theory, BC did not include a physical interpretation of the shape of the ACF decay, i.e., the flattening at short times and a more exponential decay later. We suggest that this transition between two types of behavior seen in Fig. 2 is due to the transition from ballistic to collisional behavior in the particle motion [10,12]. We discuss two pieces of evidence supporting this interpretation in the Supplemental Material [28].

V. SUMMARY

Our main result is an experimental confirmation that Belousov and Cohen's recent theory [14] accurately describes the initial decay of a time autocorrelation function for a strongly coupled plasma. The key formula developed in this theory, Eq. (1), quantitatively predicts the time dependence of the ACF decay, including its excess correlation at short times. Fitting to Eq. (1), we find that our experimental data, for a liquidlike two-dimensional strongly coupled dusty plasma, show good agreement with the theory. As an intuitive interpretation, we suggest that the transition from a flattened to a more exponential shape in the decay of the ACF is due to the transition from ballistic to collisional behavior of the microspheres [10,12], which we find happens on a timescale corresponding with the transition in the ACF.

ACKNOWLEDGMENTS

We thank Chun-Shang Wong for helpful discussions and Bin Liu for performing the supporting simulation presented in the Supplemental Material [28]. This work was supported by the US Department of Energy, the NSF, and NASA.

[1] Z. Donkó, J. Goree, P. Hartmann, and B. Liu, Phys. Rev. E **79**, 026401 (2009).
[2] S. Ichimaru, Rev. Mod. Phys. **54**, 1017 (1982).
[3] T. C. Killian, T. Pattard, T. Pohl, and J. M. Rost, Phys. Rep. **449**, 77 (2007).
[4] K. Wünsch, J. Vorberger, and D. O. Gericke, Phys. Rev. E **79**, 010201 (2009).
[5] C. K. Goertz, Rev. Geophys. **27**, 271 (1989).
[6] J.-E. Wahlund, M. André, A. I. E. Eriksson, M. Lundberg, M. Morooka, M. Shafiq, T. F. Averkamp, D. A. Gurnett, G. B. Hospodarsky, W. S. Kurth, K. S. Jacobsen, A. Pedersen, W. Farrell, S. Ratynskaia, and N. Piskunov, Planet. Space Sci. **57**, 1795 (2009).
[7] G. S. Selwyn, J. S. McKillop, K. L. Haller, and J. J. Wu, J. Vac. Sci. Technol. A **8**, 1726 (1990).
[8] S. I. Krasheninnikov, R. D. Smirnov, and D. L. Rudakov, Plasma Phys. Control. Fusion **53**, 083001 (2011).
[9] D. Chandler, *Introduction to Modern Statistical Mechanics* (Oxford University, New York, 1987), Chap. 8.
[10] M. Le Bellac, F. Mortessagne, and G. Batrouni, *Equilibrium and Non-Equilibrium Statistical Thermodynamics* (Cambridge University, New York, 2004), Chap. 9.
[11] M. Kardar, *Statistical Physics of Fields* (Cambridge University, New York, 2007), Chap. 9.
[12] P. Attard, *Non-Equilibrium Thermodynamics and Statistical Mechanics: Foundations and Applications* (Oxford University, New York, 2012), Chap. 2.
[13] L. Onsager and S. Machlup, Phys. Rev. **91**, 1505 (1953).
[14] R. Belousov and E. G. D. Cohen, Phys. Rev. E **94**, 062124 (2016).
[15] S. Machlup and L. Onsager, Phys. Rev. **91**, 1512 (1953).
[16] Z. Haralson and J. Goree, Phys. Rev. Lett. **118**, 195001 (2017).
[17] Z. Haralson and J. Goree, Phys. Plasmas **23**, 093703 (2016).
[18] Y. Feng, J. Goree, and B. Liu, Rev. Sci. Instrum. **78**, 053704 (2007).
[19] Y. Feng, J. Goree, and B. Liu, Rev. Sci. Instrum. **82**, 053707 (2011).
[20] Y. Feng, J. Goree, Z. Haralson, C.-S. Wong, A. Kananovich, and W. Li, J. Plasma Phys. **82**, 615820303 (2016).
[21] X. Wang, A. Bhattacharjee, and S. Hu, Phys. Rev. Lett. **86**, 2569 (2001).
[22] S. Nunomura, J. Goree, S. Hu, X. Wang, A. Bhattacharjee, and K. Avinash, Phys. Rev. Lett. **89**, 035001 (2002).
[23] Z. Donkó, G. J. Kalman, and P. Hartmann, J. Phys.: Condens. Matter **20**, 413101 (2008).
[24] The charge on the microspheres was also likely fluctuating on the order of ±1% around these slowly drifting average values. However, these fluctuations occurred at frequencies many orders of magnitude higher than the frequencies at which the dust particles could respond. Therefore, these fluctuations could not affect our quantity of interest, the shear stress ACF.
[25] Z. Haralson and J. Goree, IEEE Trans. Plasma Sci. **44**, 549 (2016).
[26] B. Liu, J. Goree, V. Nosenko, and L. Boufendi, Phys. Plasmas **10**, 9 (2003).
[27] P. Hartmann, G. J. Kalman, Z. Donkó, and K. Kutasi, Phys. Rev. E **72**, 026409 (2005).
[28] See Supplemental Material at http://link.aps.org/supplemental/10.1103/PhysRevE.98.023201 for additional details about the experiment, results from our other experimental runs, and further discussion of our intuitive interpretation.
[29] As a more practical way of obtaining the shear stress, instead of using the exact form of Eq. (2), we used Eq. (8b) of Ref. [17].
[30] U. Konopka, G. E. Morfill, and L. Ratke, Phys. Rev. Lett. **84**, 891 (2000).